

Nucleation and core-shell formation mechanism of self-induced $\text{In}_x\text{Al}_{1-x}\text{N}$ core-shell nanorods grown on sapphire substrates by magnetron sputter epitaxy



Ching-Lien Hsiao*, Justinas Palisaitis, Per O.Å. Persson, Muhammad Junaid, Elena Alexandra Serban, Per Sandström, Lars Hultman, Jens Birch

Thin Film Physics Division, Department of Physics, Chemistry and Biology (IFM), Linköping University, SE-581 83 Linköping, Sweden

ARTICLE INFO

Article history:

Received 21 April 2016

Accepted 22 May 2016

Available online 24 May 2016

Keywords:

InAlN

Nanorods

Nanostructures

STEM

EDX

Sputtering

MSE

ABSTRACT

Nucleation of self-induced $\text{In}_x\text{Al}_{1-x}\text{N}$ nanorod and core-shell structure formation by surface-induced phase separation have been studied at the initial growth stage. The growth of well-separated core-shell nanorods is only found in a transition temperature region ($600^\circ\text{C} \leq T \leq 800^\circ\text{C}$) in contrast to the result of thin film growth outside this region ($T < 600^\circ\text{C}$ or $T > 800^\circ\text{C}$). Formation of multiple compositional domains, due to phase separation, after ~ 20 nm $\text{In}_x\text{Al}_{1-x}\text{N}$ epilayer growth from sapphire substrate promotes the core-shell nanorod growth, showing a modified Stranski-Krastanov growth mode. The use of VN seed layer makes the initial growth of the nanorods directly at the substrate interface, revealing a Volmer-Weber growth mode. Different compositional domains are found on VN template surface to support that the phase separation takes place at the initial nucleation process and forms by a self-patterning effect. The nanorods were grown from In-rich domains and initiated the formation of core-shell nanorods due to spinodal decomposition of the $\text{In}_x\text{Al}_{1-x}\text{N}$ alloy with a composition in the miscibility gap.

© 2016 Elsevier Ltd. All rights reserved.

Semiconductor core-shell nanorods are regarded as a key building block for novel functional units exhibiting enhanced quantum efficiency (QE) as a result of large junction areas between the cores and shells compared to 2-dimensional (2D) heterojunctions [1–6]. The heterojunctions formed at non-polar sidewalls of *c*-axis oriented wurtzite semiconductor core-shell nanorods are free from the internal electric field, quantum confined Stark effect, which further benefits the QE enhancement. Ternary group III-nitride semiconductors, including $\text{In}_x\text{Ga}_{1-x}\text{N}$, $\text{Al}_x\text{Ga}_{1-x}\text{N}$, and $\text{In}_x\text{Al}_{1-x}\text{N}$ core-shell nanorods, are highly desired to apply for high-performance nanodevices [1–6]. For instance, high-brightness light-emitting devices, high-responsivity photodetectors, solar cells, and circular polarizer.

The growth of III-nitride semiconductor core-shell nanorods are mostly realized in terms of spontaneous formation of ternary alloys and intentional growth with different combinations of ternary/binary alloys using different growth techniques, such as chemical

vapor deposition (CVD), molecular-beam epitaxy (MBE), and magnetron sputter epitaxy (MSE) [1–12]. Uniform core and shell thicknesses after a mature nanorod formed are often found in the case of spontaneous formation, which can be of advantage for the device performance. Although the spontaneous formation of III-nitride core-shell nanorods were reported, most of the studies were only focused on the compositional distribution inside the nanorods using different analytical tools [7–12]. Details of how the core-shell nanorod formed from initial nucleation stage to a mature core-shell structure, and a comprehensive morphological and compositional evolutions of ternary alloys, from continuous $\text{In}_x\text{Al}_{1-x}\text{N}$ films, to core-shell nanorods, and to highly Al-rich single-phase $\text{In}_x\text{Al}_{1-x}\text{N}$ film, upon temperature and seed layer were rarely reported and discussed [7–12]. Likewise, the study of $\text{In}_x\text{Al}_{1-x}\text{N}$ core-shell nanorods is hitherto very limited in comparison with $\text{In}_x\text{Ga}_{1-x}\text{N}$ and $\text{Al}_x\text{Ga}_{1-x}\text{N}$ [1–12]. The development of $\text{In}_x\text{Al}_{1-x}\text{N}$ core-shell nanorods is very important for fabricating semiconductor nanoscale optoelectronics covering broad-optical range from infrared to ultraviolet [11–17]. Understanding the formation mechanism is needed to further control the growth of core-shell nanostructures.

* Corresponding author.

E-mail address: hcl@ifm.liu.se (C.-L. Hsiao).

In this letter, we present a study on the structural evolution of $\text{In}_x\text{Al}_{1-x}\text{N}$ nanorods from the segregation of In and Al in the early coalescence stage of film formation, epitaxially on sapphire substrates assisted with/without a VN seed layer by ultra-high-vacuum (UHV) MSE. Two different growth modes, Stranski-Krastanov and Volmer-Weber, were clearly observed in a transition temperature region in contrast to the result of thin film growth outside this region. Novel details are revealed for the formation of the self-induced core-shell nanorods at the initial nucleation stage, and their development into well-faceted hexagonal core-shell nanorods. Structural transitions from $\text{In}_x\text{Al}_{1-x}\text{N}$ epilayer or islands to core-shell nanorods predominated by phase separation is clearly presented by mass-contrast scanning transmission electron microscopy (STEM) and elemental line-profile energy dispersive x-ray spectroscopy (EDX). We also discuss effects of growth temperature and the use of seed layer on $\text{In}_x\text{Al}_{1-x}\text{N}$ morphological and compositional evolutions.

The sample growth was performed in an UHV MSE system, equipped with four magnetrons and a reflection high-energy electron diffraction (RHEED). Details of the growth system can be found elsewhere [11,12]. Two series of the $\text{In}_x\text{Al}_{1-x}\text{N}$ growth, 1) no seed layer and 2) with a vanadium nitride (VN) seed layer, on *c*-plane sapphire substrates were implemented in a temperature range of 500–900 °C, measured from thermal couple in the heater. Before the sample growth, the sapphire substrates were subsequently degreased with trichloroethylene, acetone, and isopropanol in ultrasonic baths for 5 min each and blown dry with pure nitrogen. Afterwards, the substrates were outgassed for 30 min at 1000 °C in the MSE chamber. For the samples with seed layer growth, a ~30 nm 111-orientated VN layer was deposited at 800 °C by sputtering from a V target in the same chamber. The $\text{In}_x\text{Al}_{1-x}\text{N}$ growth was cosputtered from aluminum (Al) (99.999%) and indium (In) (99.999%) targets for 20 min. The sputtering processes were carried out in a pure nitrogen (99.999999%) atmosphere at a working pressure of 5 mTorr, with a negative substrate potential of -30 V applied to the rotating substrate. DC-magnetron powers provided for Al/In targets were 300/10 and 350/9 W for the growth without and with VN seed layer, respectively. The morphology of the as-grown samples were characterized by a LEO-1550 field-emission scanning electron microscopy (FE-SEM). Analyses of structural properties and compositional profiles were performed by $\theta/2\theta$ XRD scan using a Philips 1820 Bragg-Bretano diffractometer as well as scanning transmission electron microscopy (STEM) and energy dispersive x-ray spectroscopy (EDX) using a FEI Tecnai G² TF 20 UT 200 kV FEG microscope [18,19].

Fig. 1(a) and (b) show the $\theta/2\theta$ XRD scans and FESEM images of the $\text{In}_x\text{Al}_{1-x}\text{N}$ samples directly grown on sapphire substrates, respectively. Obviously, the growth temperature influences not only alloy composition, but also morphology. As increasing the growth temperature, the $\text{In}_x\text{Al}_{1-x}\text{N}$ 0002 reflections show a transition from single peak located at 34.70°, to double peaks at 34.63° and 35.03°, and to single peak at 35.52°, corresponding to the In content, *x*, of 0.26, 0.28 and 0.20, and 0.10, for samples grown at 700, 800, and 900 °C, respectively. Here, *x* is denote to the composition of dominant phase in the $\text{In}_x\text{Al}_{1-x}\text{N}$ samples, which is determined by Vegard's rule, $x = (c_{\text{In}_x\text{Al}_{1-x}\text{N}} - c_{\text{AlN}}) / (c_{\text{InN}} - c_{\text{AlN}})$, using the measured *c* lattice constants of $\text{In}_x\text{Al}_{1-x}\text{N}$ as well as strain-free bulk AlN and InN, without considering strain effect [15,16]. Meanwhile, the morphology changes with increasing temperature from continuous thin films to nanorods, and back to thin films. The corresponding thickness measured from cross-sectional SEM are 204, 273, and 162 nm, respectively. As can be seen in Fig. 1, high-temperature film shows smoother surface (appearing atomically flat) than low-temperature film, revealing that lateral growth is enhanced at high temperature because of

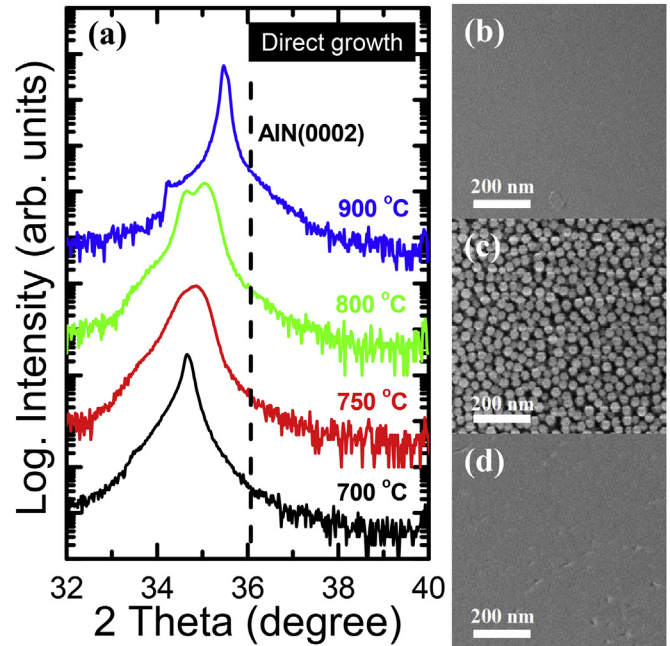


Fig. 1. (a) Temperature dependence of $\theta/2\theta$ scan XRD patterns of $\text{In}_x\text{Al}_{1-x}\text{N}$ directly grown on Al_2O_3 substrate. (b), (c), and (d) Plan-view images of the $\text{In}_x\text{Al}_{1-x}\text{N}$ grown at 900 °C, 800 °C, and 700 °C, respectively.

higher Al adatom mobility and low In incorporation towards one of the miscibility region of $x \leq 0.1$ [20,21]. At intermediate temperature region, 750–850 °C, the nanorods formed are well-separated and have a regular hexagonal shape. Since the In content of the film grown at 700 °C is in between two major phase contents of the nanorods grown at 800 °C, it implies that most of the In adatoms were incorporated into the growth not re-desorbed from the surface. This is also supported by the result of a higher growth rate of nanorods, around 133%, than the film, attributed to the effect of morphological change [14]. With increasing temperature to 900 °C, less In incorporated into the growth results in a lower growth rate, around 20%, than the film grown at 700 °C. The above results indicate that the $\text{In}_x\text{Al}_{1-x}\text{N}$ nanorod sample consists of multi-phases.

Fig. 2(a) and (b) are the $\theta/2\theta$ XRD patterns and SEM images of the $\text{In}_x\text{Al}_{1-x}\text{N}$ samples grown on VN seed layers, respectively. The trend of In content varied with growth temperature is very similar to those samples which were directly grown on sapphire, but the whole growth window is shifted to low temperature side with an around 200 °C. Almost no In was incorporated into the growth at 800 °C. The shift of growth temperature window is mainly due to higher sample surface temperatures with the VN seed layer coating. Moreover, there are some differences to the samples grown directly on sapphire substrates. The nanorods were not distributed uniformly on the VN seed layer although they were also grown well-separated with a hexagonal shape. On the other hand, the samples grown at 500 and 800 °C show granular and porous films, respectively. In addition, both $\text{In}_x\text{Al}_{1-x}\text{N}$ films and nanorods reveal lower intensity and broader linewidth of the XRD peaks, as compared to those $\text{In}_x\text{Al}_{1-x}\text{N}$ samples grown without seed layer, indicating a higher degree of misalignment along the *c* axis, poorer crystalline quality, and/or a wider compositional distribution.

The microstructural and compositional evolution of the $\text{In}_x\text{Al}_{1-x}\text{N}$ nanorods were further characterized by STEM and EDX. Fig. 3(a) shows a mass-contrast STEM micrograph of $\text{In}_x\text{Al}_{1-x}\text{N}$ nanorods grown directly on a sapphire substrate. Apparently, the

Download English Version:

<https://daneshyari.com/en/article/1689653>

Download Persian Version:

<https://daneshyari.com/article/1689653>

[Daneshyari.com](https://daneshyari.com)